SLAC-PUB-14453

Non-uniform switching of the perpendicular magnetization in a spin-torque driven magnetic nanopillar

David P. Bernstein, Björn Bräuer, Roopali Kukreja, and Joachim Stöhr

Stanford Institute for Materials and Energy Science,

SLAC National Accelerator Laboratory, Menlo Park, USA

Thomas Hauet

Institut Jean Lamour, CNRS-Nancy Université-UPV

Metz, Vandoeuvre lés Nancy, France and

Hitachi Global Storage Technologies, San Jose, USA

Julien Cucchiara and Stéphane Mangin

Institut Jean Lamour, CNRS-Nancy Université-UPV Metz, Vandoeuvre lés Nancy, France

Jordan A. Katine

Hitachi Global Storage Technologies, San Jose, USA

Tolek Tyliszczak and Kang W. Chou

Advanced Light Source, Lawrence Berkeley National Laboratory, USA

Yves Acremann

Laboratory for Solid State Physics, ETH Zurich, Switzerland

Work supported in part by US Department of Energy contract DE-AC02-76SF00515.

Abstract

Time-resolved scanning transmission x-ray microscopy (STXM) measurements were performed to study the current-induced magnetization switching mechanism in nanopillars exhibiting strong perpendicular magnetic anisotropy (PMA). This technique provides both short time (70 ps) and high spatial (25 nm) resolution. Direct imaging of the magnetization demonstrates that, after an incubation time of $\sim$ 1.3 ns, a $100 \times 300\,\mathrm{nm}^2$ ellipsoidal device switches in $\sim$ 1 ns via a central domain nucleation and opposite propagation of two domain walls towards the edges. High domain wall velocities on the order of 100 m/s are measured. Micromagnetic simulations are shown to be in good agreement with experimental results and provide insight into magnetization dynamics during the incubation and reversal period.

Spin-polarized current-induced magnetization switching (CIMS) has now been reported in many experimental works involving a wide variety of geometries including point contacts, nanopillars (spin valves or tunnel junctions) and nanowires with or without notches[20]. These systems are extensively studied, in part, because they hold potential for applications in spin transfer magnetic memory (e.g. ST-MRAM)[21]. Interest in materials with perpendicular magnetic anisotropy (PMA) has grown considerably as a pathway for lowering the critical current required to switch the magnetization while maintaining thermal stability as compared with in-plane systems[22,23]. This interest has, to a large degree, stemmed from calculations of the switching behavior using a macrospin approximation[24]. Although reproducible ultrafast switching with high effciency has been demonstrated[25], the macrospin model has not been consistent with all experimental results.

To fully understand CIMS dynamic phenomena in PMA materials, two time scales need to be considered: a long time scale dominated by thermal activation[26,27] and a short time scale dominated by angular momentum conservation[25,26]. Early studies on spin-transfer in PMA-based devices have been devoted to a description of quasi-static phenomena on longer time scales. Only very recent experiments have used time resolved transport measurement with current pulses as short as 300 ps[25,26].

In this Rapid Communication, we present the results obtained by studying the CIMS mechanism in PMA nanopillars at nanometer length scales and picosecond time scales using scanning transmission X-ray microscopy (STXM) images taken while injecting a spin polarized current. These images are further compared with micromagnetic simulations. We demonstrate that, in $100 \times 300\,\mathrm{nm}^2$ devices, CIMS starts with pre-switching dynamics that result in the nucleation of a reversed magnetic domain. The switching mechanism is completed by two domain walls propagating in opposite direction and their subsequent annihilation at the edge of the pillar. The delay time, domain nucleation and domain wall propagation are discussed. A domain wall velocity of $\sim 100\,\mathrm{m/s}$ is measured and shown to be consistent with micromagnetic simulations[28].

The multilayer samples were deposited by DC magnetron sputtering at 2 mTorr Ar pressure onto ambient temperature Si wafers coated with Si_3N_4. The reference and free magnetic layers of the sample stack are Pd(2 nm)/[Co(0.29 nm)/Pd(0.8 nm)]$\times$ 5/[Co(0.2 nm)/Ni(0.7 nm)]$\times$ 2/Co(0.2 nm) and [Co(0.2 nm)/Ni(0.7 nm)]$\times$5/Co(0.2 nm), respectively. A 4 nm Cu spacer layer was deposited to ensure a magnetic decoupling between the two magnetic layers. Top

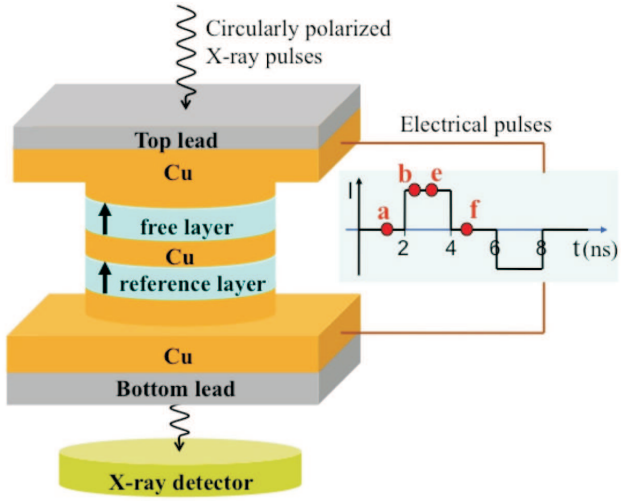

FIG. 1. (Color Online) Schematic of the Scanning Transmission X-ray microscopy (STXM) experiment performed on a [Co/Ni] based nanopillar spin valve. The pulse sequence (current versus time) is shown on the right. Letters (a), (b), (d) and (f) represent, respectively, the STXM measurements corresponding to the images shown in Fig. (2)

and bottom leads are respectively Ta/Cu (50 nm) and Cu(15 nm)/Ta(3 nm). The multilayer film was then patterned using electron beam lithography and ion etching to form $100\times300\,\mathrm{nm}^2$ nanopillars with an ellipsoidal shape. A last chemical etching step was performed on the sample backside to open a $200 \times 200\,\mathrm{nm}^2$ window in the Si wafer. The spin-torque devices sit in the center of this window on a 300 nm thick Si_3N_4 membrane chosen for its transparency to x-rays. The samples were finally mounted to custom printed circuit board sample holders and wire-bonded to SMA connectors so that current pulses could be injected.

In order to image the magnetization reversal process, the scanning transmission x-ray microscope (STXM) available on beamline 11.0.2 at the Advanced Light Source (ALS) was used. Images of the spatially resolved magnetic contrast with an time resolution of 70 ps were obtained as described in[29–32]. Beamline 11.0.2 is equipped with an elliptically polarized undulator (EPU) capable of providing arbitrary circular or linear polarization. In our experiment, the incident beam was parallel to the surface normal (as show in Fig. (1) and focused by a zone plate with a 25 nm resolution. The photon energy is tuned to the characteristic Ni L_3 resonance edge. Note that Ni is present in both free and reference layer but 2.5 times more in quantity in the free layer. In the following, we consider the magnetic configuration

of the high anisotropy reference layer uniform and fixed, as confirmed by the simulation.The experiment is repeated for both left- and right-circular polarizations to provide a magnetic contrast through the x-ray magnetic circular dichroism (XMCD) effect[33]. The experiment provides, for one specific element (nickel in our case), a measurement of the magnetization component parallel to the incident light direction, i.e. along the PMA axis.

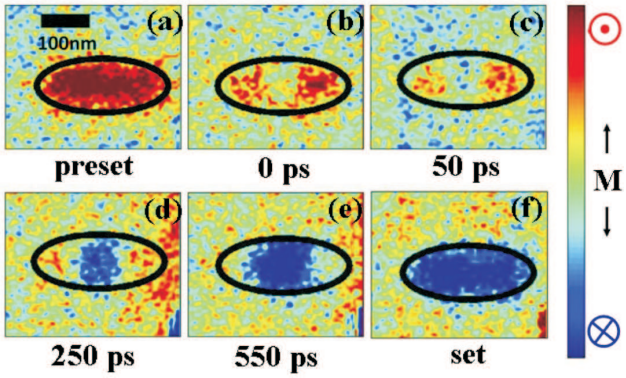

FIG. 2. (Color) Experimental STXM images of the magnetic contrast in a $100 \times 300\,\mathrm{nm}^2$ ellipsoidal nanopillar spin valve. Images (a) to (e) have been taken at different times during the CIMS reversal based on the setup shown in Fig. (1). Image (a) is the initial state and (f) the final state. The color scale corresponds to the perpendicular component of the free layer magnetization, from parallel (red) to anti-parallel (blue) with respect to the reference layer.

A critical feature of our experimental setup is the ability to synchronize the current pulses to the bunch structure of the ALS ring within a precision of 70 ps, yielding the time resolution of our experiment[29,30]. As presented in Fig. (1), the current pulse sequence was applied as follow: 4 ns positive or "set" pulse/4 ns no current/ 4 ns negative or "reset" pulse/ 4 ns no current. Voltages of ± 748 mV were applied during the set and reset pulses, respectively, corresponding to a current density of $\sim 5 \times 10^7\,\mathrm{A/cm^2}$. The rise time of the current pulses was 100 ps. By varying the delay between the x-ray probe and the current pulses, we were able to measure the time evolution of the magnetization. Fig. (2) shows a typical switching event as electrons travelled from the free layer to the reference layer. The imaged CIMS process therefore corresponds to the free layer magnetization switching from a parallel to an anti-parallel alignment with respect to the reference layer magnetization. The experiment was carried out at room temperature and in absence of magnetic field.

The "preset" image on Fig. (2a) shows the free layer magnetization state before a current

pulse is injected into the structure. Images shown in Fig. (2) are obtained by accumulating data while repeating the method described above. It is important to note that, since our experiment uses STXM in a pump-probe mode, the images show the perpendicular component of the Ni sublattice magnetization averaged over a large number of pulse sequences. As a consequence of the averaging, this method does not allow us to identify stochastic processes. Fig. (2b) shows that the sample undergoes a so-called "incubation" time during which the pillar is subjected to a spin polarized current but the free layer has not started to reverse its magnetic orientation[34,35]. After this incubation time a central region of the pillar starts reversing. This region of nucleation appears more clearly after 50 ps in Fig. (2c). Times quoted in Fig. (2) are given with respect to the first observed domain nucleation (Fig. (2b)) because of a possible offset in the absolute time. In other words, the precision on the pulse onset time does not allow us to quantify the 1.3 ns incubation time with a better precision than 300 ps. The relative times, however, are accurate within the quoted time resolution. In Fig. (2d) and Fig. (2e) the reversed domain grows by domain wall motion towards the edges. In Fig. (2e), at 550 ps, the sample magnetization has not fully switched yet. An image taken in between the set pulse and the reset pulse confirms the total saturation of the sample (Fig. (2f)). The present data set offers direct proof of incoherency in the short time regime CIMS. It provides explanation for the discrepancies between macrospin model and very recent time resolved macroscopic transport measurements performed on similar PMA devices[25–27].

To get a deeper understanding of the magnetization reversal, we performed a 3D micromagnetic calculation of the Landau Lifshitz Gilbert (LLG) equation using the Scheinfein code[36] where the injected current pulse was taken into account in the Slonczewski spin-torque term[37]. The calculations performed considered a $100 \times 300\,\mathrm{nm}^2$ ellipsoidal element mimicking the same stack as described above where the reference layer is divided into 3750 cells and the soft layer into 1875 cells. The free-layer parameters were $\mathrm{M}_s = 650\,\mathrm{emu/cm}^3$ ($0.650\,\mathrm{A/m}$) and $\mathrm{K}_u = 2.7 \times 10^6\,\mathrm{erg/cm}^3$ ($2.7 \times 10^5\,\mathrm{J/m}^3$). The reference layer had a saturation magnetization $\mathrm{M}_s = 500\,\mathrm{emu/cm}^3$ and its magnetization was kept fixed along the anisotropy axis perpendicular to the film plane. The intra-layer exchange coupling between cells is $2\,\mu$erg (20 pJ/m) (for both layers), the current polarization is $p = 0.35$ and the damping coefficient is $\alpha = 0.1$[22]. Temperature was taken into account within an initial 5 degree tilt of the free layer magnetization. Current duration and amplitude were 4 ns and

15 mA, respectively. The electrons were injected from the free to the hard layer starting with a parallel initial configuration. A sequence of those simulations is shown in Fig (3).

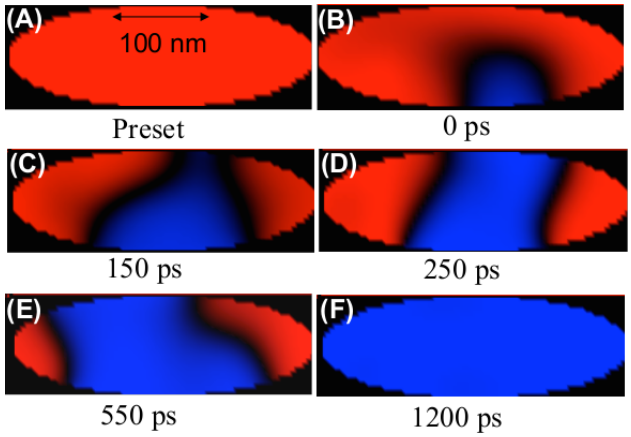

FIG. 3. (Color) Series of micromagnetic simulation showing the free layer configuration at different times (a) to (f) during the CIMS process in a $100 \times 300\,\mathrm{nm}^2$ PMA nanopillar. The color scale is the same as in Fig 2 and corresponds to the perpendicular component of the free layer magnetization, from parallel (red) to anti-parallel (blue) with respect to the reference layer. Times are given with respect to domain nucleation

The micromagnetic simulations shown in Fig. 3(a) to (g) and the experimental STXM results are in good qualitative agreement. The simulated incubation time and switching time are 1.3 ns and 1.2 ns, respectively. The size of the nucleated domain is smaller than $50 \times 50\,\mathrm{nm}^2$ and the domain wall width is of the order of 20 nm. The simulated domain walls are Bloch-like walls but this information is not experimentally confirmed because the STXM spatial resolution is about 25 nm. Rough calculations based on successive experimental images in Fig. (2c), (2d) and (2e), as well as simulated results, lead to a domain wall propagation speed of the order of 100 m/s. While fast domain wall speeds have been observed in Co/Pt/AlOx systems, the results presented here are achieved with 5 orders of magnitude less current density[28,38]. Note that simulations show a more dissymmetric nucleation and domain wall propagation (Fig.3) than in the experimental images (Fig. (2)). However, such behavior may be artificially wiped out by the pump-probe nature of the measurements. The position of the magnetization nucleation inside the free layer must result from the addition of the dipolar field originating from the reference layer on the free layer and the free layer internal demagnetization field. Indeed starting from a parallel configuration of the

layer magnetizations, both these dipolar and demagnetization fields favor a magnetization reversal at the ellipse center. On the contrary, we can here note that, starting from the AP state, the nucleation may occur at the edge of the ellipse as favoured by the dipolar field in this configuration. The relative amplitude of the dipolar and demagnetization field has then to be quantified.

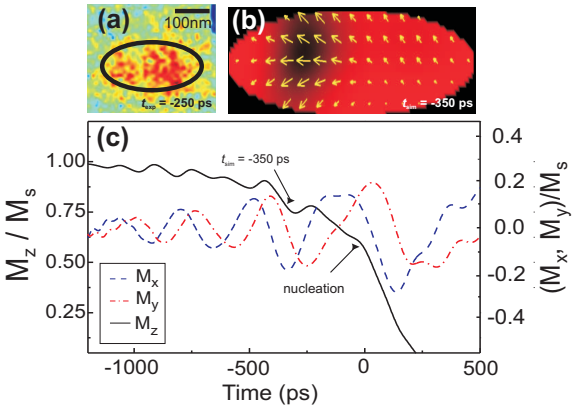

FIG. 4. (Color) (a) Experimental image of the magnetization along the PMA axis in the free layer at -250 ps where the color scale ranges from parallel (red) to anti-parallel (blue) and the negative sign indicates that the image was taken prior to nucleation. (b) The simulated magnetization in the free layer at -350 ps where the length of the yellow arrows corresponds to the amplitude of the in-plane magnetic component. (c) Simulated component of the magnetization along PMA direction (M_z, left vertical axis) as well as the two in-plane components (M_x and M_y, right vertical axis).

Finally, information on the free layer magnetic behaviour during the incubation time can be extracted from comparison between STXM data and simulation. Simulations in Fig. 4(c) show the out-of-plane (M_z) and in-plane (M_x, M_y) components of the free layer magnetization during the incubation time. The pre-nucleation dynamics features are a small amplitude oscillatory behaviour of M_z correlated to dephased M_x and M_y component oscillations. M_x and M_y oscillation amplitude increases continuously until domain nucleation is reached. Such evolution is typical of a current-induced magnetization precession that leads to switching over a certain magnetization tilt angle. The precessional modes may be uniform[24] or non-uniform[35]. Fig.4(a) corresponds to a STXM image taken at -250 ps where the minus sign indicates that the image was taken prior to the nucleation. The component of magnetization along the PMA axis is undoubtedly non-uniform over the pillar area when compared with the

preset image (Fig.2(a)). This experimental result is well described within the simulations. A symptomatic case of the non-uniformity during the incubation time dynamics is shown in Fig.4(b). Although all the simulated spins precess as the current is turned on, a localized area of larger amplitude precession is observed that is continuously displaced during the incubation time and ultimately results in nucleation within that region.

In conclusion, by using the nanometer scale resolution of Scanning Transmission X-ray microscopy (STXM) measurements combined with time resolution given by the ALS ring, we were able to investigate current-induced magnetization switching (CIMS) dynamics driven by polarized current pulses in a perpendicularly magnetized (PMA) sample. We observed that the fast switching is highly nonuniform for a $100 \times 300\,\mathrm{nm}^2$, ellipse. The STXM observations are well supported using a micromagnetic calculation. Comparison with simulations provide the details of magnetization dynamics and nucleation/propagation process which occur during the magnetization switching. The non-uniformities observed in the magnetization during the incubation time and as the switching occurs explain the previously reported discrepancies between experimental results and the macrospin model[25,26]. Future experiments designed to study the impact of nonuniform magnetization on the switching speed and thermal stability are needed as these are critical features in the development of ST-RAM applications.

Acknowledgements: The authors would like to acknowledge Olav Hellwig for his help with PMA deposition process, H. Tomita, Y. Suzuki, A. Kent and E.E. Fullerton for discussions, and the U.S. Department of Energy, Office of Science, Office of Basic Energy Science for its continued support under contract DE-AC02-76SF00515. B.B. acknolwedges support from the German Research Foundation (DFG). The Advanced Light Source is supported by the Director, Office of Science, Office of Basic Energy Sciences, of the U.S. Department of Energy under Contract No. DE-AC02-05CH11231.

---

[20] D. Ralph and M. Stiles, Journal of Magnetism and Magnetic Materials, **320**, 1190 (2008), ISSN 0304-8853.

[21] J. Katine and E. E. Fullerton, Journal of Magnetism and Magnetic Materials, **320**, 1217 (2008), ISSN 0304-8853.

[22] S. Mangin, D. Ravelosona, J. A. Katine, M. J. Carey, B. D. Terris, and E. E. Fullerton, Nat. Mater., **5**, 210.

[23] S. Mangin, Y. Henry, D. Ravelosona, J. A. Katine, and E. E. Fullerton, Applied Physics Letters, **94**, 012502 (2009).

[24] J. Z. Sun, Phys. Rev. B, **62**, 570 (2000).

[25] D. Bedau, H. Liu, J.-J. Bouzaglou, A. D. Kent, J. Z. Sun, J. A. Katine, E. E. Fullerton, and S. Mangin, Applied Physics Letters, **96**, 022514 (2010).

[26] D. Bedau, H. Liu, J. Z. Sun, J. A. Katine, E. E. Fullerton, S. Mangin, and A. D. Kent, Applied Physics Letters, **97**, 262502 (2010).

[27] J. Cucchiara, Y. Henry, D. Ravelosona, D. Lacour, E. E. Fullerton, J. A. Katine, and S. Mangin, Applied Physics Letters, **94**, 102503 (2009).

[28] T. A. Moore, I. M. Miron, G. Gaudin, G. Serret, S. Auffret, B. Rodmacq, A. Schuhl, S. Pizzini, J. Vogel, and M. Bonfim, Applied Physics Letters, **93**, 262504 (2008).

[29] Y. Acremann, V. Chembrolu, J. P. Strachan, T. Tyliszczak, and J. Stohr, Review of Scientific Instruments, **78**, 014702 (2007).

[30] J. P. Strachan, V. Chembrolu, X. W. Yu, T. Tyliszczak, and Y. Acremann, Review of Scientific Instruments, **78**, 054703 (2007).

[31] Y. Acremann, J. P. Strachan, V. Chembrolu, S. D. Andrews, T. Tyliszczak, J. A. Katine, M. J. Carey, B. M. Clemens, H. C. Siegmann, and J. Stöhr, Phys. Rev. Lett., **96**, 217202 (2006).

[32] J. P. Strachan, V. Chembrolu, Y. Acremann, X. W. Yu, A. A. Tulapurkar, T. Tyliszczak, J. A. Katine, M. J. Carey, M. R. Scheinfein, H. C. Siegmann, and J. Stöhr, Phys. Rev. Lett., **100**, 247201 (2008).

[33] G. Schütz, W. Wagner, W. Wilhelm, P. Kienle, R. Zeller, R. Frahm, and G. Materlik, Phys. Rev. Lett., **58**, 737 (1987).

[34] T. Devolder, J. Hayakawa, K. Ito, H. Takahashi, S. Ikeda, P. Crozat, N. Zerounian, J.-V. Kim, C. Chappert, and H. Ohno, Phys. Rev. Lett., **100**, 057206 (2008).

[35] Y.-T. Cui, G. Finocchio, C. Wang, J. A. Katine, R. A. Buhrman, and D. C. Ralph, Phys. Rev. Lett., **104**, 097201 (2010).

[36] "Llg micromagnetic simulator developed by prof. m. scheinfein, http://llgmicro.home.mindspring.com,".

[37] J. C. Slonczewski, Journal of Magnetism and Magnetic Materials, **159**, L1 (1996), ISSN 0304-

8853.

[38] T. Koyama, G. Yamada, H. Tanigawa, S. Kasai, N. Ohshima, S. Fukami, N. Ishiwata, Y. Nakatani, and T. Ono, Applied Physics Express, **1**, 101303 (2008)

[20] D. Ralph and M. Stiles, Journal of Magnetism and Magnetic Materials, **320**, 1190 (2008), ISSN 0304-8853.

[21] J. Katine and E. E. Fullerton, Journal of Magnetism and Magnetic Materials, **320**, 1217 (2008), ISSN 0304-8853.

[22] S. Mangin, D. Ravelosona, J. A. Katine, M. J. Carey, B. D. Terris, and E. E. Fullerton, Nat. Mater., **5**, 210.

[23] S. Mangin, Y. Henry, D. Ravelosona, J. A. Katine, and E. E. Fullerton, Applied Physics Letters, **94**, 012502 (2009).

[24] J. Z. Sun, Phys. Rev. B, **62**, 570 (2000).

[25] D. Bedau, H. Liu, J.-J. Bouzaglou, A. D. Kent, J. Z. Sun, J. A. Katine, E. E. Fullerton, and S. Mangin, Applied Physics Letters, **96**, 022514 (2010).

[26] D. Bedau, H. Liu, J. Z. Sun, J. A. Katine, E. E. Fullerton, S. Mangin, and A. D. Kent, Applied Physics Letters, **97**, 262502 (2010).

[27] J. Cucchiara, Y. Henry, D. Ravelosona, D. Lacour, E. E. Fullerton, J. A. Katine, and S. Mangin, Applied Physics Letters, **94**, 102503 (2009).

[28] T. A. Moore, I. M. Miron, G. Gaudin, G. Serret, S. Auffret, B. Rodmacq, A. Schuhl, S. Pizzini, J. Vogel, and M. Bonfim, Applied Physics Letters, **93**, 262504 (2008).

[29] Y. Acremann, V. Chembrolu, J. P. Strachan, T. Tyliszczak, and J. Stohr, Review of Scientific Instruments, **78**, 014702 (2007).

[30] J. P. Strachan, V. Chembrolu, X. W. Yu, T. Tyliszczak, and Y. Acremann, Review of Scientific Instruments, **78**, 054703 (2007).

[31] Y. Acremann, J. P. Strachan, V. Chembrolu, S. D. Andrews, T. Tyliszczak, J. A. Katine, M. J. Carey, B. M. Clemens, H. C. Siegmann, and J. Stöhr, Phys. Rev. Lett., **96**, 217202 (2006).

[32] J. P. Strachan, V. Chembrolu, Y. Acremann, X. W. Yu, A. A. Tulapurkar, T. Tyliszczak, J. A. Katine, M. J. Carey, M. R. Scheinfein, H. C. Siegmann, and J. Stöhr, Phys. Rev. Lett., **100**, 247201 (2008).

[33] G. Schütz, W. Wagner, W. Wilhelm, P. Kienle, R. Zeller, R. Frahm, and G. Materlik, Phys. Rev. Lett., **58**, 737 (1987).

[34] T. Devolder, J. Hayakawa, K. Ito, H. Takahashi, S. Ikeda, P. Crozat, N. Zerounian, J.-V. Kim, C. Chappert, and H. Ohno, Phys. Rev. Lett., **100**, 057206 (2008).

[35] Y.-T. Cui, G. Finocchio, C. Wang, J. A. Katine, R. A. Buhrman, and D. C. Ralph, Phys. Rev. Lett., **104**, 097201 (2010).

[36] "Llg micromagnetic simulator developed by prof. m. scheinfein, http://llgmicro.home.mindspring.com,".

[37] J. C. Slonczewski, Journal of Magnetism and Magnetic Materials, **159**, L1 (1996), ISSN 0304-8853.

[38] T. Koyama, G. Yamada, H. Tanigawa, S. Kasai, N. Ohshima, S. Fukami, N. Ishiwata, Y. Nakatani, and T. Ono, Applied Physics Express, **1**, 101303 (2008).